

WAKES OF ROTORCRAFT MANEUVERING IN GROUND EFFECT

Anthony Huang
School of Aerospace Engineering
AE8900
Summer/2001

Advisor: Professor N.M. Komerath

Advisor's Signature: _____

Date: _____

Grade: _____

Abstract

The aerodynamic characteristics of rotorcraft maneuvering in ground effect are investigated to better understand and quantify the flow field structures and unsteadiness associated with various in ground effect flight conditions. The computational modeling to simulate in ground effect in hover and forward flight is being developed. These prediction models will be refined and validated with experimental results. Experimental investigations will involve flow visualization, velocity, pressure, and loads measurements aimed at examining the airflow and wake behavior associated with in ground effect. A literature study of the past research pertaining to ground effect flows has been conducted, including influences on the flow fields, rotor induced velocity, force and moment variations, tip vortex geometry, and ground vortex formation due to the ground. A simple analytical calculation has been performed to estimate the time scales for the blade tip vortex to reach the ground and recirculate back to the rotor. For robust prediction models to exist, a good agreement between measured, computed, and analytical results is essential.

1. Introduction

The behavior of rotor wake in the vicinity of the ground is challenging to predict. Under in ground effect (IGE) conditions, the wake would collide with the ground and cause a significant perturbation to the flow near the blade. Significant interactions between the main rotor wake and the ground have been associated with the formation and passage of the ground vortex in transitional flight. If a helicopter encounters a ground vortex, the main rotor may be forced to provide additional power and the stability of the aircraft is degraded.

A research task titled “Wakes of Rotorcraft Maneuvering in Ground Effect” has been conducted at Georgia Tech since January 2001 under the Rotorcraft Center of Excellence program. The aim of this research is to capture the physics of the flow features and dynamics of ground effect flows around rotorcraft, provide an understanding of the behavior of rotor wakes/vortices near the ground, and generate rigorous analytical models to predict Handling Qualities. The aerodynamic models will be refined through experiments, analysis, computation, and basic physical modeling. Specific issues in the analytical modeling, relevant to Handling Qualities prediction include:

- Effect of ground on vortex strength
- Effect of ground on blade loads
- Modification of rotor inflow due to wake distortion and ground.
- Moments on rotor disk due to ground
- Moments on fuselage due to ground
- Deflection of wake due to fuselage and ground
- Influence of axial flow in vortex
- Time lag effects on inflow and loads due to time scales of ground vortex unsteadiness and wake response.

2. Objectives

The objectives of this research are to:

1. Develop physically-based models for the behavior of rotor wakes in ground effect, with unsteadiness due to maneuvers.
2. Understand time scales of unsteadiness, including the genesis, structure and evolution of the ground vortex, as well as vortex-vortex interactions as wakes distort.
3. Use the findings to improve the aerodynamics in reduced-order flight simulation models.

The goal of the first part of this study is to determine the rotor wake distortion due to ground effect and quantify the velocity and pressure fields through wind tunnel experiments.

3. Background/Literature Review

3.1 Flow Fields

In a wind tunnel experiment with a rotor, the boundary conditions on the wall or ground plane are not a representative of a helicopter flying near the ground. Instead, they are representative of a helicopter hovering with ambient wind. If a precise simulation of a helicopter flying near the ground is needed, proper boundary conditions need to be met. This may be achieved by using a moving ground or a treadmill in the wind tunnel or by employing unique test facilities such as the Princeton Dynamic Model Track. In the Princeton Track, models were moved through still air on a servo-controlled carriage in an enclosed building, and hence proper simulation of the ground boundary conditions was obtained.

In helicopter translational flight near the ground two distinct flow regimes occur: recirculation of the rotor wake at low end of advance ratio range, and a ground vortex formed as the advance ratio increases, causing irregular changes in the hub moments with advance ratio¹. The flow phenomenon is presented in Figure 1. With IGE, there is a significant additional downward flow through the forward half of the rotor².

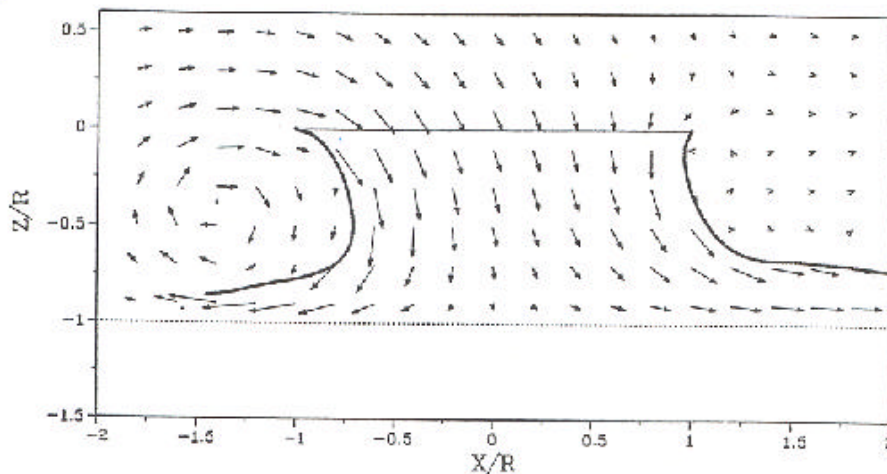


Figure 1: Velocity vector plot of a typical case with ground vortex.

At low advance ratio a recirculation regime where part of the wake flows forward and upward and recirculates through the lifting rotor occurs. There is little lateral flow and moderate level of unsteadiness in the flow field¹. Periodical fluctuation of interference flow between downwash and upwash due to flow re-circulation introduces the unsteady phenomena³. The flow field fluctuates at a rather low frequency². Above a critical advance ratio, which depends upon collective pitch and height-to-diameter ratio, a well-defined concentrated horseshoe vortex is formed under the rotor, and significant lateral

flow is present. The flow field becomes quite steady. The vortex becomes smaller and smaller and eventually vanished as the advance ratio is increased.

The existence of these flow regimes can be characterized by a dimensionless parameter $\mu^* = \mu/\sqrt{(C_T/2)}$ as might be expected from momentum theory considerations². That is, from momentum theory this single parameter determines the gross characteristics of the wake, i.e., the wake deflection angle. Reference [4] states that the helicopter flow field is approximately the same at equal values of non-dimensional speed, μ^* , for a given dimensionless ground height h/R . The flow velocity at each flow field point varies with time, due to the rotation of the blades and the associated passage of the wake elements by the field points. The significant time variation of the flow velocity near the wake boundary is mostly due to periodic passage of the tip vortices past the point on the rocket trajectory.

3.2 Rotor Induced Velocity

When a helicopter is operating closely and entirely above a steady and horizontal solid plane larger than the rotor disk, the major influence of ground proximity can be viewed as a reduction of the average induced velocity at the rotor disk³.

In the forward and middle part of the rotor the induced velocity distribution varies greatly with the advance ratio. The induced velocity distribution varies with the ground height in all part of the rotor. The variation in the front part is caused by the effect of the ground vortex, whereas the variation in the rear part is caused by the effect of the ground plane, which is equivalent to adding an upward velocity to the rotor disk⁵.

3.3 Ground Vortex

A ground vortex can be formed by the interaction between the main rotor downwash and the incoming wind in close proximity to the ground. When rotors are operating near the ground at low advanced ratios, the forward part of rotor wake, after impinging on the ground plane, will flow forward and then roll up, forming a ground vortex around the rotors, as shown in Figure 2. For a single rotor, the ground vortex center in the longitudinal symmetric plane is a little upstream of rotor leading edge⁵. When the ground vortex approaches the leading edge of the main rotor, it induces large downwash on the rotor disk. Consequently the thrust is reduced. The ground vortex also alters the helicopter yaw control effectiveness in sideway and rearward flights near the ground.

The shape of the ground vortex looks like a half circle attached to two trailing vortices, similar to a horseshoe vortex with a large core. The ground vortex strength is sensitive to the wake decay rate, an input parameter depending on both the rotor height above the ground and the wind speed⁶.

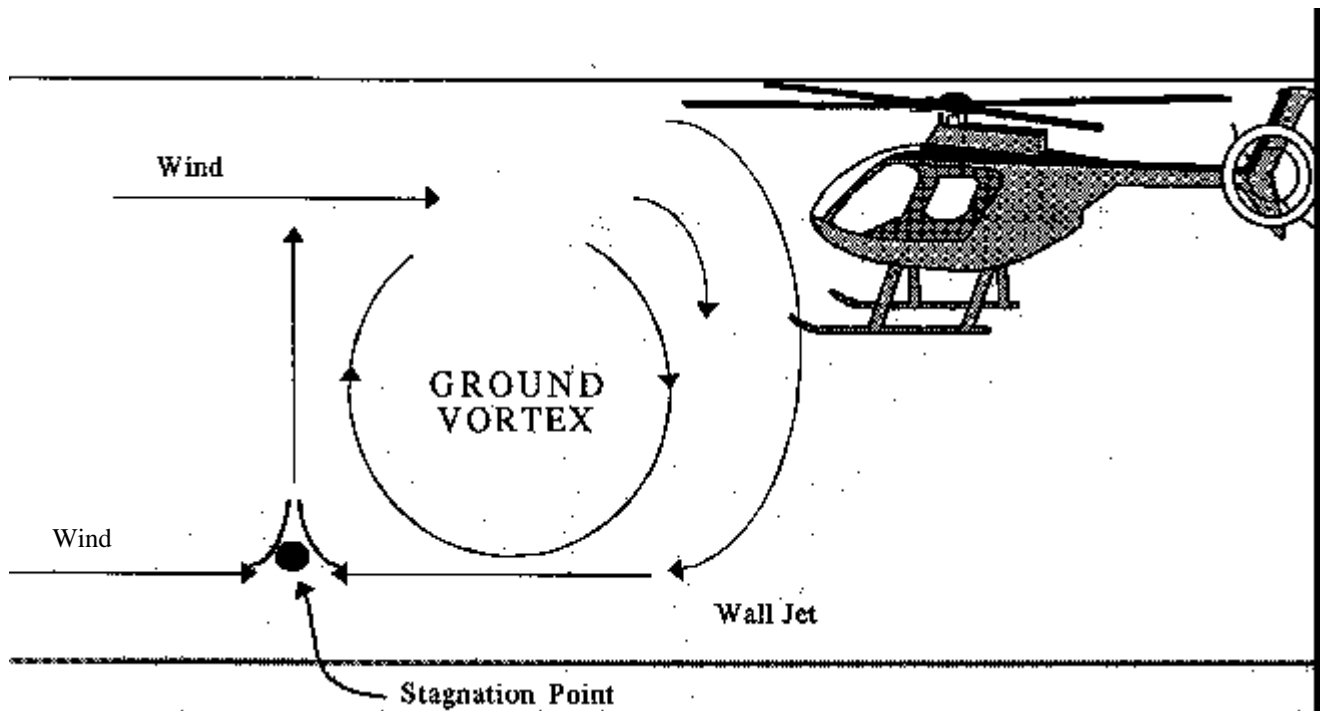


Figure 2 Ground vortex structural characteristics

The ground vortex itself is quite unsteady, both in size and shape, and also in location⁷. The ground vortex has a large-scale low-frequency pulsating behavior, which is referred to as puffing of the ground vortex. The sequence of this puffing behavior is as follows. First the ground vortex is very small, but growing. For slow forward speed or for hover in light winds, the ground vortex would stay upstream. As the wind velocity increases, the ground vortex moves closer to the rotor. Interaction between the old vortices and new vortices increases as forward airspeed increases. As the ground vortex continues to grow, it eventually becomes too large for the flowfield to sustain. At this point the entire flowfield breaks up violently, and the large ground vortex is swept downstream. Immediately a new small ground vortex begins to grow upstream, and the cyclic process repeats itself⁸.

The presence of a vortex near the ground plane will induce unsteady separation within the viscous boundary layer on the ground plane. This unsteady separation phenomenon results in the formation of a jet of fluid directed away from the ground plane and which affects the tip vortices shed from the rotor.

Increasing advance ratio moves the ground vortex further aft under the rotor. Increasing collective pitch and/or reducing height-to-diameter ratio moves the ground vortex forward¹. With a greater height above the ground, the ground vortex emerges and disappears both at a smaller advance ratio⁵.

As described in Reference 2, the order of magnitude of the ground vortex strength can be estimated by modeling an elementary ground vortex as a line vortex and adding it to the flow field computed by the method described in Reference 9. This estimate results in a vortex strength given by:

$$\Gamma_{GV} \cong 4\mathbf{p} \cdot h_v V$$

where h_v is the height of the vortex above the ground. Reference 2 provides equations for estimate of the ground vortex strength.

$$\frac{\Gamma_{GV}}{\Gamma_w} = 2\mathbf{p} \left(\frac{h_v}{h} \right) \mathbf{m}^* v^*$$

where $\mathbf{m}^* = \mathbf{m} \sqrt{2/C_T}$ normalized advance ratio

$v^* = \frac{v}{\Omega R} \sqrt{\frac{2}{C_T}}$ normalized induced velocity

For the experiment in Reference 2, $\frac{h_v}{h} \approx 0.5$ and $\mathbf{m}^* v^* \approx 0.5$. Therefore $\frac{\Gamma_{GV}}{\Gamma_w} \approx 1.6$.

The estimates of the ground vortex strength indicate that it is at least an order of magnitude stronger than the tip vortex².

3.4 Forces & Moments

With IGE large and irregular changes in the hub moments occur over a narrow advance ratio range. The forces and moments in ground effect are very sensitive to low levels of translational acceleration and deceleration indicating that the ground effect experienced by helicopters is sensitive to the nature of the flight path¹. Under accelerating conditions the ground vortex apparently does not become fully established. The effects are quite large at the low ground height.

Force and moment variation over an advance ratio range is largely a consequence of the distortion of the wake. The thrust coefficient decreases with advance ratio from hover due to recirculation and then begins to rise as advance ratio continues to increase. The torque remains relatively constant. The hub pitching moment remains relatively constant up to an advance ratio and then begins to increase¹. This increase is associated with the formation of the ground vortex. The recirculation promotes a downflow at the leading edge of the rotor due to wake distortion and delays development of longitudinal inflow distribution characteristics of operation out of ground effect. As the ground vortex forms it acts to rapidly push the leading edge of the wake upwards and reduces the inflow at the leading edge of the rotor resulting in rapidly increasing nose up moments with advance

ratio. A lower height-to-diameter ratio increases the irregular variations in the thrust and moment with advance ratio.

3.5 Tip Vortex Geometry

The ground plane significantly alters the tip vortex geometry. This is most significant in the radial location of the tip vortex¹⁰. With IGE, the wake contracts for a short period, then expands rapidly. This is in sharp contrast to the OGE tip vortex geometry. The radial data of measurements made in Reference 10 show more apparent scatter in the far wake than was evident in the axial data. This suggests that the rotor wake is more unsteady in the radial direction than in the axial direction.

In hover, tip vortices in the wake boundary are transported downward, whereas in low speed forward flight the tip vortices travel inboard and slightly above the rotor and are then transported down through the rotor disk¹¹.

The rotor/ground plane separation distance has a much greater influence on the tip vortex radial location. The tip vortices at different h/R have a similar initial contraction rate. However, the smaller separation distance between the rotor and ground plane causes the tip vortex expansion to begin sooner after the initial contraction, and the expansion occurs at a faster rate¹⁰. On the other hand, the ground plane has very little effect on the tip vortex axial location in the near wake. However, the effect becomes significant near the ground plane. The axial descent rate decreases as the vortex approaches the ground plane and reaches zero very close to the ground.

4. Technical Approach

The behavior of a rotor wake in the vicinity of a ground plane will be studied, including the origin and development of the ground vortex, the flow in the boundary layer under the wake, and the flow in and around a mature ground vortex. The computation will be supported by experiments aimed at identifying the major features of the interaction of the wake with the ground plane and determining the flowfields. Flow visualization is a very important tool in understanding the physics of the flow field. Pulsed laser sheet visualization will be used to capture both qualitatively and quantitatively the structure and dynamics of vortex interaction with the ground plane, flow in the boundary layer under the wake vortex, and the evolution of the ground vortex structures.

The rotor wake in close proximity to a ground plane is highly unsteady with the helical vortices comprising the wake being distorted in shape and even destroyed by collision with the ground plane. The magnitude of the axial velocity within the vortex determines the intensity of the interaction.

Of particular interest is the dynamic behavior of the rotor as a result of high positive or negative inflows to the rotor disk caused by the ground vortex. The inflow above the rotor tip-path-plane will be quantified with velocity measurements to see if there is any

correlation between the inflow change and unsteady phenomenon downstream. Some time delay may be expected.

The experiment will be conducted in the GT 7' × 9' wind tunnel for various ground height with a static ground plane. A flat plate acting as the ground plane will be translated vertically in the tunnel to interact with the wake of a 2-bladed rotor.

Velocity measurements will be conducted to quantify the differences in the wake produced by the ground effect. Since the flowfield is highly three-dimensional and unsteady, this will require a combination of measurement approaches involving Spatial Correlation Velocimetry (SCV), Particle Image Velocimetry (PIV), Laser Doppler Velocimetry (LDV), and hot wire anemometry techniques. Different techniques will be employed to capture different phenomena in different regions.

Pressure fluctuations will be measured at different locations on the ground surface with microphones flush mounted on the ground plate. This will quantify pressure unsteadiness and the time scales of such unsteadiness.

IGE rotor-fuselage experiments will be performed with three different generic fuselage shapes. In addition to the flow visualization and velocity and pressure measurements as performed for the isolated rotor, forces and moments on the fuselage model will be measured. Beside the ground height, an additional parameter, yawing angle, will be incorporated as a variable. Simple representations of the forces and moments on these generic shapes will be developed, so that force/moment predictions for other shapes can be generalized from a combination of these.

More specifically the experimental investigations are broken into subtasks in three year period as in the following:

Year 1: Wake distortion and velocity field determination

1. An isolated 2-bladed model will be operated over a range of low advanced ratios for various heights above a ground plane in the wind tunnel. The experiments with a static ground plane simulate the rotorcraft hovering above the ground with ambient wind.
2. Empirical relations for wake distortion due to ground effect will be developed by image analysis of laser sheet videography. A wake-boundary tracking algorithm will be developed to standardize the procedure for obtaining wake skew angles in both longitudinal and lateral planes.
3. Velocity field measurements, which involves PIV, LDV, SCV and hot-wire anemometry techniques, will be conducted to quantify the differences in the wake produced by ground effect. The regions and phenomena to be captured using different techniques will be determined.
4. Pressure fluctuations at the vortex interaction regions on the ground surface will be measured with microphones mounted on the ground surface. This is to quantify pressure unsteadiness.

Year 2: Load measurements on generic fuselage shapes

1. IGE rotor experiment will be repeated with a generic force-instrumented tapered circular-cylinder fuselage.
2. Forces and moments on the fuselage model will be measured with varied yawing angle and ground height.
3. Two more generic fuselages will be developed: an ellipsoid + tailboom shape and a square-section shape.
4. Unsteadiness/time scales will be quantified in terms of blade frequency and other relevant parameters.
5. Velocity measurements will be made to understand the reasons for variations in fuselage loads. These may include capturing flow separation regions and velocity field differences due to unsteady phenomena using a combination of LDV and SCV. Image analysis using laser sheet may also be needed for examining wake distortion.

Year 3: Determination of time lag in inflow and loads

1. Time/phase lag effects in the fuselage forces and moments will be quantified for the 3 generic fuselage shapes.
2. Time scales in the velocity fields will be measured.
3. General representations of the forces and moments on these generic shapes will be developed, so that predictions can be made for other shapes.

5. Experiment

The experiments aim at identifying the basic physical phenomenon of the ground vortex and major features of the interaction of the wake with the ground plane.

5.1 Facility

The experiments will be conducted in the John J. Harper 7' × 9' wind tunnel. It is a closed circuit, single return, atmospheric wind tunnel, driven by a 600 HP electric motor. The speed in the test section can be continuously varied up to 220 ft/s.

The rotor is a two-bladed teetering rotor, with a 18" (.457m) radius. The blade has a NACA0015 airfoil section with a constant chord of 0.0857m (3.374"). The blade is untwisted with a fixed collective pitch of 10°. Rotor rotation is counter-clockwise when viewed from the top. The rotor shaft is tilted at 6° to simulate forward flight. For this experiment, the rotor will be run at an RPM of 1050 and/or 2100 for all measurements and flow visualization. The advance ratio will initially be set to 0.1 in the tests. Measurements made from the past experiment as shown in reference 12 indicates that the rotor has a thrust coefficient $C_T = 0.005825$ at the advanced ratio $\mu = 0.0$, $C_T = 0.008231$ at

$\mu= 0.075$, and $C_T= 0.008271$ at $\mu= 0.1$ when the rotor is far above the ground plane. It should be noted that when the rotor operates close to the ground, the thrust coefficient might not be the same due to the ground effect.

The ground plane will be made of a rectangular aluminum flat plate, which needs to be thick enough to prevent vibration and long enough to capture ground vortex interaction downstream during the test. Since continuous motion of the moving ground plane is not required, the vertical translation of the ground plane will be made manually with some joint structure underneath the plate. It must be ensured that the joint mechanism provides firm, stable linkage between the plate and the tunnel ground surface and hence fluttering of the plate is minimized when the tunnel is on.

5.2 Test Conditions

The flow visualization, velocity field measurement, and pressure field measurement experiments will be conducted with the test condition listed below first. All parameters will be kept constant except the ground height initially. After the major flow characteristics for the baseline condition are identified, the rotor speed may be increased to 2100 rpm and the advance ratio may be changed up or down to compare phenomena produced for different conditions if found necessary.

Hover at 1050 RPM with 16.6 ft/s cross-wind (advance ratio = 0.1)

- a) Maximum ground height
- b) 1 rotor diameter ground height ($h/D=1$)
- c) 1 rotor radius ground height ($h/D=0.5$)
- d) 0.75 rotor radius ground height ($h/D=0.375$)

5.3 Diagnostic Techniques

5.3.1 Flow Visualization

5.3.1.1 Surface tuft flow visualization

Surface tufts are to be used to investigate the flow field near the ground plane. These tufts are white cotton threads that need to be cut into approximately 3 cm lengths and fixed to the ground plane with cyanoacrylate glue. They will be oriented in the downstream direction initially and spaced 1.5” apart in both chordwise and spanwise directions. Marks are to be drawn on the ground to indicate rotor radius for assisting geometry identification. The ground plane will be illuminated with incandescent lights and visualization will be recorded to a video tape during tunnel run. This visualization will be used to identify the vortex interaction region and determine surface flow direction in the wake interaction region.

5.3.1.2 Laser Sheet Flow Visualization

The technique is used to visualize flow patterns in both streamwise and spanwise vertical planes and observe the wake geometry, vortex/surface interaction and vortex trajectories near the surface. The laser sheet optics is to be placed downstream in the test section or on the side of the tunnel and directed into the test section, depending on whether streamwise or lateral flow patterns are captured. The position of the laser sheet will be varied during the test by moving the laser sheet optics in order to keep the laser sheet parallel or perpendicular to the freestream direction. The streamwise laser sheets will be placed at spanwise stations $y/R = 0, \pm 0.33, \pm 0.66$, and the spanwise sheets will be placed in the vortex interaction regions, which will be identified from the surface tuft flow visualization. An azimuth disk, used to determine vortex age, will be mixed into the video signal. Flow seeding will be generated with a set of nichrome smoke wires strung from the floor to the ceiling in the upstream of the tunnel test section. The wires will be wrapped with cotton twine, coated with wax, and heated with a variable transformer to produce smoke in the test. The flow images will be recorded with an intensified CCD video camera. A grid board is to be recorded in the laser sheet location before the test in order to aid identifying coordinates for later analysis.

A Metalaser Technologies copper vapor pulsed laser rated at 30 watts will be used. It can run at pulse rates between 4000 and 8000 Hz and has a 75 ns pulse width. The short pulse width is ideal for flow visualization because it freezes an instantaneous flow picture. The laser output is directed into the test section through a fiber optic cable. For these tests the laser will be run at 5994 Hz, which is a multiple of the 29.97 Hz framing rate of NTSC standard video camera. The camera used to capture images will be placed perpendicular to the plane of the light sheet. The video will be digitized using MediaRecorder on the SGI-02 workstation.

5.3.2 Velocity Measurements

Various velocity measurement techniques will be used to quantify the steady and time-varying structure of the rotor wake and ground vortex.

Large-area flow velocity fields will be captured using SCV. For high resolution over small areas, PIV will be used. In regions of periodic velocity variation where high accuracy is needed, such as quantifying rotor inflow, LDV will be used. In regions where the time scales of fluctuations must be captured, hot-wire measurements will be conducted. Both SCV and PIV provide 2-component velocity information in a plane, while LDV provides up to 3-component velocity information at a single point.

5.3.2.1 Spatial Correlation Velocimetry

SCV is a planar velocity measurement technique that quantifies velocity from the information contained in planar flow visualization. It computes the displacement between two images of the flow from their cross-correlation function. The basic premise of the technique is that most of the energy of the flow is contained in the larger “packets” of

fluid. These “packets,” imaged with sufficiently small time delay, remain largely undistorted, exhibiting a spatial displacement. Therefore flow velocities are determined by measuring displacement between two images of seeding patterns. By obtaining images close together in time, the velocities can be assumed to be instantaneous. Thus unsteady flows can be captured.

The methodology is as follows – a light sheet is used to illuminate a single plane in a flow field. Intensified cameras are used to image seeding moving through this light sheet. Two images separated by a small time are digitized from the two cameras and then subdivided into small sub-image regions, and a spatial cross-correlation is performed on the corresponding sub-image regions from each image. The resolution values for images depend on video camera resolution. Sub-images are generally 64×64 pixels. Images are normally delayed by 8 pixels. The displacement of the peak of the cross-correlation function from the origin indicates the spatial shift in the seeding patterns. The computed velocity represents the average velocity of all the seeding particles in that sub-image. The calculation is repeated for each sub-image area to determine velocities in the imaged plane. Since SCV computes an average of the displacements of all particles in a correlation window, it is ideally suited for large rotorcraft flowfields where resolution of very small scale motion is not critical.

When SCV is used, it must be ensured that the velocity component not being measured, termed the 3rd component, is not much higher than the other two components. In a three-dimensional flow, the seeding will not only be moving within the plane of illumination but will also be moving perpendicular to it. Thus the patterns in the plane of illumination must not move out of that plane between images.

The detailed description of SCV technique can be found in Reference 13.

5.3.2.2 Particle Image Velocimetry

PIV is another well established, non-intrusive technique for the measurement of mean and instantaneous fluid velocity in a plane of interest. In PIV techniques, the displacement between peaks of the spatial autocorrelation of double-pulsed images is computed. The sign of the displacement vector is determined through additional instrumentation such as rotating mirrors, color or polarization differences between the two laser pulses¹⁴.

Since PIV requires the identification of particles, there must be particles in all regions of interest. In a wind tunnel test, it is expected that at any given instant there will be various regions with no seeding. Thus PIV is limited to small areas. Implementation of PIV also requires sharp particle images. To obtain accurate autocorrelations or fringes, particles must not be smeared, which places severe restrictions on the lighting and imaging requirements.

In general, PIV method remains confined to a small area by the need to use seed particles which are small enough to follow while being large enough so that their scattering can be resolved.

5.3.2.3 Laser Doppler Velocimetry

Another non-intrusive measurement technique widely used is LDV. It is a point-wise technique capable of measuring up to 3 velocity components at a single point. The main principle of LDV is that when a moving particle passes through the fringe patterns formed by intersecting coherent light beams the resulting Doppler shift frequency of the scattered light is proportional to the velocity of the particle¹³. Although LDV is precise, this method is time consuming when applied over large areas. Thus, it should be restricted to regions where high accuracy of periodic velocity variation is needed.

5.3.2.4 Hot wire anemometry

The hot wire anemometry measurements will be conducted at several points to obtain more quantitative information about the unsteadiness of the flowfield. The anemometry is a highly sensitive, fast responding device capable of detecting small, rapid fluctuations in velocity without time lag. When the hot wire is used, the wire is kept heated by an electric current to a temperature between 200 and 300 °C. When air flows over the wire, energy in the form of heat is carried away by the much colder air stream, resulting a change in voltage. This voltage change is used to calculate the change in air velocity.

5.3.3 Pressure Measurements

Unsteady pressures measurements will be made using B&K Falcon Model #4939 1/4" condenser microphones. In order to reduce complexity of data acquisition and analysis, the maximum number of microphones used in the test will be limited to four at a time. These microphones will be flush mounted on the ground surface plate. Numerous holes will be drilled in the ground plate with equal spacing in between each other, so microphones can be moved around to locations of interest during the test. The calibration coefficient for each microphone will need to be determined from an acoustical calibrator at 114 dB at 1 kHz and checked against those provided by B&K. In the experiment the data will be sampled thousands of times of rotor frequency and averaged over each degree of blade rotation. The unsteady pressure coefficient variation with rotor azimuth will then be determined from the microphone data.

6. Analytical Solution

Recirculation of the rotor wake or tip vortices may have significant influences on the unsteadiness of the flowfield as discussed previously. Preliminary calculations have been performed to estimate the time scales for the rotor tip vortices to reach the ground plane and re-circulate back to the rotor disk using a simple method. The analysis is mainly concerned with determination of vortex descent rate. Given the ground height, the time

for the tip vortex to reach the ground can be determined once the vortex descent rate is known.

The first step of analysis involves calculating the inflow ratio and wake induced velocity using momentum theory for hover and Glauert momentum theory for forward flight.

In hover,
$$I_i = \sqrt{\frac{C_T}{2}}$$

In forward flight,
$$C_T = 2\sqrt{m^2 + (m \cdot \tan \alpha + I_i)^2} \cdot I_i$$

$$v_i = I_i \cdot \Omega R$$

Both equations above for calculating the inflow ratio requires thrust coefficient. Since C_T with IGE is unavailable, C_T (OGE) are used assuming that the values do not vary greatly from C_T (IGE) and are good enough for estimates.

Momentum theory assumes uniform rotor inflow across the entire disk. In reality, the induced velocity is minimum at the root and maximum at the tip. To simplify the problem, it is assumed to vary linearly from zero at the rotor hub to a maximum at the tip, as shown in Figure 3. Applying conservation of mass, the maximum induced velocity at the blade tip can be determined as a relationship with the uniform induced velocity predicted by momentum theory.

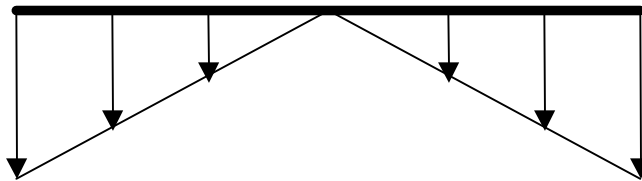


Figure 3 Rotor induced velocity profile

$$\dot{m} = \text{const} = r \cdot A \cdot v_i$$

For uniform inflow,
$$\dot{m} = r \cdot (v_i)_{avg} (\rho R^2)$$

For linearly varying inflow, $\dot{m} = \int_{r=0}^{r=R} 2\mathbf{p} \cdot \frac{(v_i)_{\max}}{R} r \cdot dr = \frac{2\mathbf{p}}{3} r(v_i)_{\max} R^2$

$$\Rightarrow r \cdot (v_i)_{\text{avg}} (\mathbf{p}R^2) = \frac{2\mathbf{p}}{3} r(v_i)_{\max} R^2$$

$$\Rightarrow (v_i)_{\max} = \frac{3}{2} (v_i)_{\text{avg}}$$

As the fluid just outboard the tip vortices is close to stationary, tip vortices are assumed to descent at half the rate of the maximum induced velocity (average velocity of fluid just inboard and outboard the tip vortices). The geometry of the tip vortices with rotor wake is presented in Figure 4. For simplicity, the descent rate is assumed constant as vortices move towards the ground. Thus the time for the tip vortex to reach the ground is simply the ground height divided by the vortex descent rate.

For calculating the time for the tip vortex to recirculate back to the rotor disk from the ground surface, conservation of mass theory is used again. Since mass of fluid going down through the rotor is equal to mass of fluid going up through the sides of the tunnel, as shown in Figure 5, the rate at which the fluid recirculates up can be determined.

$$\dot{m} = r \cdot (\mathbf{p}R^2) \cdot (v_i)_{\text{avg}} = r \cdot (d \times w - \mathbf{p}R^2) \cdot v_{up}$$

$$v_{up} = \frac{(\mathbf{p}R^2)}{(d \times w - \mathbf{p}R^2)} \cdot (v_i)_{\text{avg}}$$

where w = width of tunnel test section = 9'
 d = rotor disk diameter = 3'

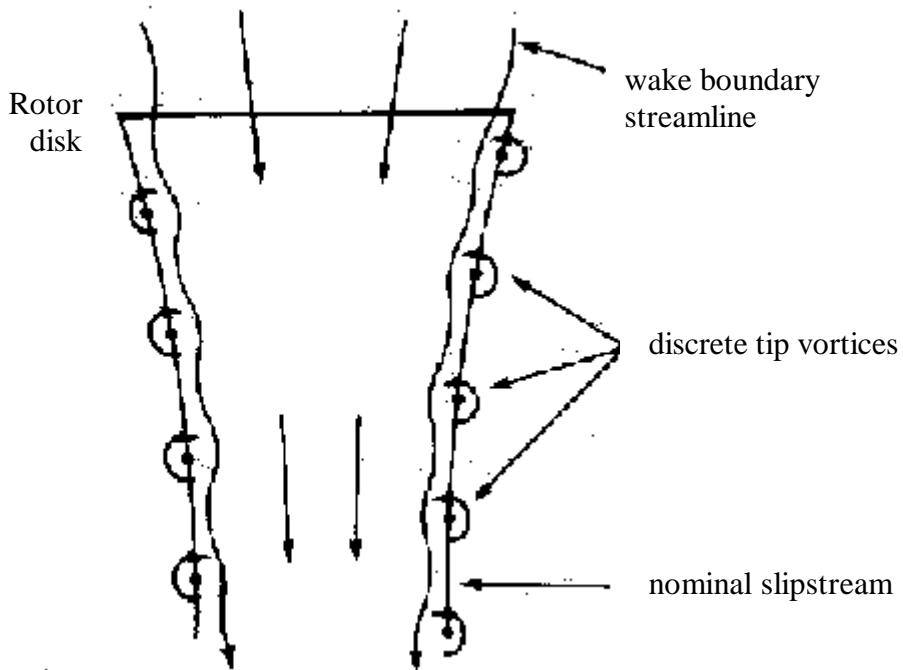


Figure 4 Geometry of rotor wakes and tip vortices

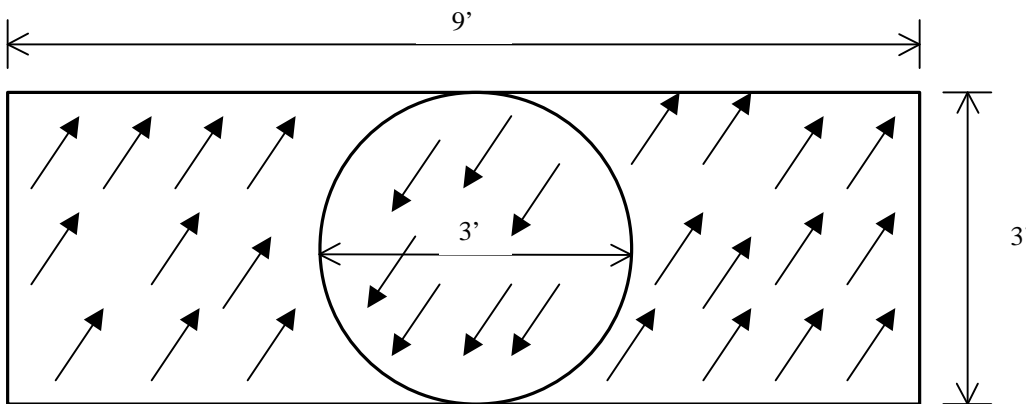


Figure 5 Recirculation of rotor wakes

Knowing upward recirculation speed, the time for the tip vortex to recirculate back to the rotor can be found now. The summation of these two time scales is the period of tip vortex recirculation.

The following two tables show sample calculations for rotor in hovering and forward flight (both at 1050 rpm). The time scale of the tip vortex recirculation for one rotor radius ground height is within 1 second and is simply doubled as the ground height is doubled. This is due to simplification made in our calculations that the thrust coefficient is independent with the ground height and hence the induced velocity is kept constant. Tip vortex recirculation takes longer in forward flight than in hovering, because the wake induced velocity in forward flight condition is lower than in hovering. From the simple estimates, it can be concluded that the time scale of the period of recirculation is in the order of 1~2 seconds for $h/R=1$ and 2. The detailed calculations performed in a spreadsheet is presented in Appendix A.

Hovering

h/R ground height	t1 (s) downward	t2 (s) upward	t (s) total
1	0.22593	0.47518	0.70111
2	0.45186	0.95035	1.40221

Forward flight ($\mu = 0.1$)

h/R	t1 (s) downward	t2 (s) upward	t (s) total
1	0.25497	0.53626	0.79123
2	0.50994	1.07252	1.58246

7. Conclusions and Recommendations

It is well known that the rotorcraft may experience handling problems in IGE condition. This task is to develop detailed physics-based modeling to capture the essential features of ground-effect flows and their effects on rotorcraft. Experimental study will be carried out at Georgia Tech with computational analysis performed at The Ohio State University. The results of this work will determine the important parameters in the modeling of ground effect flows. Success criteria comprise successful experimental measurements, validated reduced-order analytical models, simplified models for use in comprehensive rotor codes, and good agreement between measured and computed results.

A literature research including effects due to the ground on the flow fields, rotor induced velocity, force and moment variations, tip vortex geometry, and ground vortex formation has been conducted. Preliminary planning of experiments has been performed. Development of computer codes for IGE simulation is in process. The first tunnel entry involving flow imaging experiments with isolated rotor and varying ground plane height will be in the coming months. GenHel code will be obtained to perform baseline comparisons.

It has been observed that under some IGE conditions the behavior of flows is different for hovering flight with ambient wind and forward flight in still air. Blowing near the surface

or a moving ground experiments will need to be incorporated into the task proposed and explored at a later stage to identify reasons for differences between the two types of flight conditions.

References

1. Curtiss Jr., H.C., Erdman, W., and Sun, M., "Ground Effect Aerodynamics", International Conference on Rotorcraft Basic Research, 1985.
2. Curtiss, H.C. Jr., Sun, M., Putman, W.F., Hanker, E.J. Jr., "Rotor Aerodynamics in Ground Effect at Low Advance Ratios", Journal AHS, Jan 1984.
3. Xin, H., "Development and Validation of a Generalized Ground Effect Model for Lifting Rotors", PhD Thesis, Georgia Tech, 1999.
4. Hanker, E.J. Jr. and Smith, R.P., "Parameters Affecting Helicopter Interactional Aerodynamics in Ground Effect", Journal AHS, Jan 1985.
5. Kang, N. and Sun, M., "Simulated Flowfields in Near-Ground Operation of Single- and Twin-Rotor Configurations", Journal of Aircraft, Vol.37, No. 2, Mar-Apr 2000.
6. Lee, C.S. and He, C.J., "A Free Wake/Ground Vortex Model For Rotors At Low Speed In-Ground-Effect Flight", 51st AHS Annual Forum, 1995, Proceedings. Vol. 1.
7. Cimbala, J.M., Billet, M.L., Gaublotme, D.P., and Oefelein, "Experiments on the Unsteadiness Associated with a Ground Vortex", Journal of Aircraft, Apr 1991.
8. Saberi, H.A. and Maisel, M.D., "A Free-Wake Rotor Analysis Including Ground Effect", Annual Forum Proceedings- 43rd American Helicopter Society.
9. Heyson, H.H., "Linearized Theory of Wind Tunnel Jet Boundary Corrections and Ground Effect for VTOL-STOL aircraft", NASA TR R-124, 1962.
10. Light, J.S., "Tip Vortex Geometry of a Hovering Helicopter Rotor in Ground Effect", Journal of the American helicopter Society, Apr 1993.
11. Landgrebe, A.J., Taylor, R.B., Egolf, T.A., and Bennett, J.C., "Helicopter Airflow and Wake Characteristics for Low Speed and Hovering Flight", Journal AHS, Oct 1982.
12. Brand, A.G., "An Experimental Investigation of the Interaction Between a model Rotor and Airframe in Forward Flight", PhD Thesis, Georgia Tech, Mar 1989.
13. Fawcett, P.A., "An Investigation on Planar Velocimetry by Spatial Cross Correlation", PhD Thesis, Georgia Tech, Mar 1992.
14. Reddy, U.C., "Whole Field Velocity Measurements in Three-Dimensional Periodic Flows", PhD Thesis, Georgia Tech, Mar 1999.

Appendix A - Simple Estimates for Time Scales of Vortex Recirculation

μ	0	0.1
$C_T(\text{OGE})$	0.005825	0.008271

Omega	1050	rpm
	109.9557	rad/s
R	1.5	ft
C	0.281167	ft
σ	0.119331	
A	6.3	per rad
θ	10	deg
α_{tpp}	6	deg
h/R	1	
H	1.5	ft
D	3	ft
W	9	ft

Hover

$\mu = 0$

λ	0.053968	
v_i	8.901068	ft/s
v_{i_max}	13.3516	ft/s
v	6.675801	ft/s
t1 (down)	0.22593	s
v_up	3.156722	s
t2 (up)	0.475176	s
t (total)	0.701106	s

Forward Flight

$\mu = 0.1$

λ	0.03731	
C_T	0.008271	
$C_T - C_T$	3.26E-07	
λ_{tpp}	0.04782	
v_i	7.887203	ft/s
v_{i_max}	11.8308	ft/s
v	5.915402	ft/s
t1	0.254972	s
v_up	2.79716	ft/s
t2 (up)	0.536258	s
t (total)	0.79123	s